Available online at www.sciencedirect.com
SCIENCE DIRECT®
International Journal of Pharmaceutics 298 (2005) 186–197
international journal of pharmaceutics
www.elsevier.com/locate/ijpharm

Structural characteristics and crystal polymorphism of three local anaesthetic bases Crystal polymorphism of local anaesthetic drugs: Part VII

A.C. Schmidt *

Institute of Pharmacy, Ph. Technology, University of Innsbruck, Innrain 52, 6020 Innsbruck, Austria

Received 1 December 2004; received in revised form 25 April 2005; accepted 25 April 2005

Abstract

Benzocaine (BZC), butambene (BTN) and isobutambene (BTI) are basic local anaesthetic agents of the ester type, preferentially used for surgery and dental procedures. The compounds, official in the USP (BZC and BTN) and Ph. Eur. (BZC), were each found to exist in two polymorphic crystal forms and their solid state characteristics have been determined by thermomicroscopy, differential scanning calorimetry (DSC), FTIR-, FT-Raman-spectroscopy as well as X-ray powder diffractometry. This work further emphasizes the comparison of solid state characteristics of three compounds with closely related structural features on molecular level, leading to opportunities for the investigation of structure-property relationships. Mod. I^0 is the particular thermodynamically stable form at room temperature in all of the three systems. This form is present in commercial products and can be crystallized from solvents at room conditions. Mod. II can be obtained by annealing the supercooled melt or fast cooling of a saturated solution, respectively. The endothermic transformation of mod. II to mod. I^0 upon heating confirms that mod. I^0 is thermodynamically stable at ambient conditions (heat of transition rule) whereas mod. II is enantiotropically related to mod. I^0, i.e. is metastable at temperatures above the transition temperature. The metastable forms show different kinetic stabilities at room temperature.

Keywords: Local anaesthetics; Crystal forms; Crystal polymorphism; Thermal analysis; Hot-stage microscopy; Solid state properties

1. Introduction

Local anaesthetics (LA) of a general formula lip–CO–hydr (lip: lipophilic end, mostly phenyl ring; CO: negatively charged linkage, commonly ester or amide; hydr: hydrophilic group, tertiary or secondary amine) are representatives of a drug class well known for the formation of polymorphs and solvates (Giron et al., 1997; Borka and Haleblian, 1990). The hydrophilic group is responsible for the receptor binding whereas the lipophilic and the linking group

* Tel.: +43 512 507 5370; fax: +43 512 507 2933.
E-mail address: andrea.schmidt@uibk.ac.at.

0378-5173/$ – see front matter © 2005 Elsevier B.V. All rights reserved.
doi:10.1016/j.ijpharm.2005.04.025

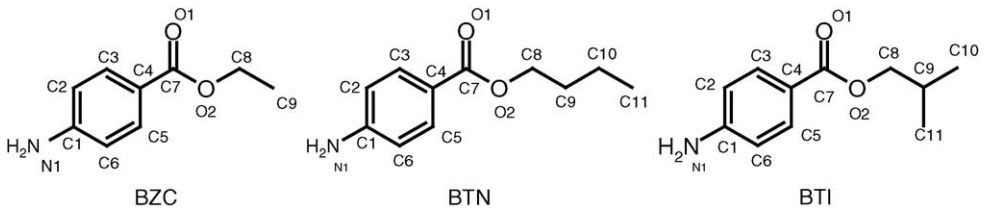

Fig. 1. Molecular structure of three local anaesthetic bases benzocaine (BZC), butambene (BTN), isobutambene (BTI) with atomic numbers.

affect the duration of action (Goodman and Gilman, 1998).

The present paper deals with the solid state characterization and phenomena of crystal polymorphism of three local anaesthetic basic compounds (Fig. 1), which cause reversible local loss of feeling before and during surgery, dental procedures (including dental surgery) or labor and delivery. They generally are used in topical compositions and methods for treating pain (Williams and Zhang, 2003). Benzocaine (BZC) and isobutambene (BTI) moreover are used in sunscreen lotions as UV-absorbing active compounds with a Sunscreen Index (SI) at a medium level of 9.6 (BZC), 9.2 (BTI), 8 (BTN) determined at an optical density of 3.080 Å in a concentration of 1% (Boyle et al., 2002). BZC is official in the European (Ph. Eur.) and the US Pharmacopoeia (USP) and BTN only is official in the USP. BTI, mainly used in cosmetics, is not official in any pharmacopeia. The structural related methyl *p*-hydroxybenzoate was one of the earliest being recognized as organic polymorphic compound showing six polymorphs (Lindpaintner, 1939; Kofler and Kofler, 1954; Kuhnert-Brandstätter, 1971) and the crystal structure of the stable form (monoclinic) was solved with crystals grown from organic solution (Zhengdong et al., 1997). Thus, we expected the structural relatives BTN and BTI to be polymorphic, too.

The existence of polymorphic crystal forms of BTN and BTI has not been mentioned in any of the previous analytical studies dealing with the solid state properties of these compounds. The stable crystal form of BTN was determined to be monoclinic (Watanabe, 2002). BZC was found to be dimorphic (Gruno et al., 1993) and the crystal structure of the stable form was solved (Baptista, 1968; Sinha and Pattabhi, 1987) as orthorhombic ($P2_12_12_1$) and revised (Lynch and McClenaghan, 2002) with crystals grown from an ethanolic solution being also monoclinic ($P2_1/c$). They all agree that the compound comprises a flat molecule arranged, head to tail, in linear ribbon arrays via a N–H···O=C association as found in some other local anaesthetics.

In the present study, we describe the formation, the physical properties and similarities of polymorphic behaviour of the structural related BZC, BTN and BTI by thermal analytical methods, vibrational spectroscopy, powder X-ray diffraction and water-vapor sorption analysis evaluating their relative thermodynamic and kinetic stabilities. Although the other analytical methods indicate a strong relationship between the three compounds, X-ray studies show different crystal systems.

2. Materials and methods

2.1. Materials

BZC: four samples of benzocaine ("uk aus H_2O/ether 10/77", "Dr. E. Ritsert's Anaesthesin AMNG", "Anästhesin Benzocain INN", "Benzocaine B.P. Herba") were available for this study. BTN/BTI: "Butamben EC No. 202-317-1 Lot 99H2514" and "Cycloform Curta & Co. Berlin-Britz 941249" were used. All solvents used in this study were of p.a. ("pro analysis") quality.

2.2. Methods

2.2.1. Hot-stage microscopy

The thermal behaviour of the solid state forms was observed using a Olympus BH-2 polarizing microscope (Olympus Optical Co. Ltd.) equipped with a Kofler hot-stage (Reichert, Vienna, A) and linked with a digital camera (Olympus DP50, Olympus Optical Co. Ltd.) using AnalySIS® Image Processing software.

2.2.2. Differential scanning calorimetry (DSC)

DSC-thermograms were recorded with a DSC 7 system (Perkin-Elmer, Norwalk, CT, USA) using the Pyris 2.0 software. Samples of approximately 2 mg (weights controlled to ±0.0005 mg using a UM3 ultra-microbalance, Mettler, Greifensee, CH) were weighed into Al-Pans (25 μl) with perforated cover. Dry nitrogen was used as purge gas (purge: 20 ml min^{-1}). Low-temperature DSC-curves were recorded with a DSC 7 (Perkin-Elmer), head temperature −80 °C. Both were calibrated with caffeine (236.4 °C) and indium 99.999% (156.6 °C, 28.45 J/g).

2.2.3. Thermal gravimetric analysis

TGA-7 (Perkin-Elmer), sample weights 3–5 mg, Al-pans (50 μl), N_2 (sample purge: 20 ml/min).

2.2.4. Infrared-spectroscopy

Fourier transform infrared (FTIR)-spectra were acquired on a Bruker IFS 25 spectrometer (Bruker Analytische Messtechnik GmbH, Karlsruhe, D). Spectra over a range of 4000–400 cm^{-1} with a resolution of 2 cm^{-1} (50 scans) were recorded on KBr tablets (approximately 2 mg PRCHC per 300 mg KBr). For temperature-controlled FTIR-spectra the samples were prepared on ZnSe disks using a heating device (Bruker) and the Bruker IR microscope I (Bruker Analytische Messtechnik GmbH), with 15×-Cassegrain-objectives (spectral range 4000–600 cm^{-1}, resolution 4 cm^{-1}, 100 interferograms per spectrum).

2.2.5. Raman-spectroscopy

Raman-spectra were recorded with a Bruker RFS 100 Raman spectrometer (Bruker Analytische Messtechnik GmbH), equipped with a Nd:YAG Laser (1064 nm) as excitation source and a liquid-nitrogen-cooled, high-sensitivity Ge-detector. The spectra were recorded in aluminium sample holders at a laser power of 300 mW (64 scans per spectrum).

2.2.6. Powder X-ray diffractometry (PXRD)

The X-ray diffraction patterns were obtained using a Siemens D-5000 diffractometer (Siemens AG, Karlsruhe, D) equipped with a theta/theta goniometer, a Goebel mirror (Bruker AXS, Karlsruhe, D), a 0.15° soller slit collimator and a scintillation counter. The patterns were recorded at a tube voltage of 40 kV and a tube current of 35 mA, applying a scan rate of 0.005° 2θ s^{-1} in the angular range of 2°–40° in 2θ. Temperature- and moisture-controlled experiments were done with a low-temperature camera TTK (Anton Paar KG, Graz, A) and a SYCOS-H humidity control system (Asynco, Karlsruhe, D).

2.2.7. Water-vapor sorption analysis

The moisture sorption isotherms were acquired using a SPS-11 moisture sorption analyzer (MD Messtechnik, Ulm, D). The measurement cycles were started at 0% relative humidity (RH) and increased in 10% steps up to 90% RH and back to 0% RH. The equilibrium condition for each step was set to a weight constance of ±0.007% over 40 min. The temperature was 25 ± 0.1 °C.

3. Results and discussion

The crystal forms are named according to the Kofler notation (Kofler and Kofler, 1954) using roman numerals in the order of the melting points (i.e. the form with the highest melting point is called mod. I). The modification which is thermodynamically stable at 20 °C is marked with a superscript zero.

3.1. Preparation of the polymorphic crystal phases

BZC: Mod. I^0, the thermodynamically stable form at room temperature, is present in commercial products and crystallizes from all organic solvents tested in this study, such as ethanol, ethanol 70%, methanol, 1-propanol, 2-propanol, 1-butanol, 1-pentanol, acetone, acetonitrile, methylene chloride, trichlormethylene, diethyl ether, ethyl acetate, *n*-hexane, cyclohexane, 1,4-dioxane, nitromethane, ethyl methyl ketone, dimethyl formamide, toluene and from the melt at temperatures above 65 °C. Mod. II can be crystallized by quenching a saturated solution of BZC in 1-butanol at −8 °C (Gruno et al., 1993) and from the supercooled melt below 64 °C.

BTN: Mod. I^0 is present in commercial products and crystallizes from all organic solvents tested in this study and from the melt at temperatures above 45 °C. Mod. II can be crystallized from the supercooled melt below 45 °C.

BTI: Mod. I^0 is present in commercial products and crystallizes from all organic solvents tested in this study

and from the melt at temperatures above 45 °C. Mod. II can be crystallized from the supercooled melt below 45 °C.

All of the three unstable crystal forms occur on quenching the melt or the solution, respectively, according to Ostwald's Rule of Stages (Ostwald, 1897). Recrystallization from the solvents mentioned above did not lead to solvent adducts (pseudopolymorphs), as expected from former investigations on local anaesthetics of the ester type (Schmidt, in press-b).

3.2. Characterization of the polymorphic crystal phases

3.2.1. Thermal analysis

Hot-stage microscopy—BZC: The commercial product consists of polyedric (100–200 μm), highly birefringent crystals of the stable form mod. I^0 with a strong secondary texture. On heating up to 80 °C using a heating rate of 5 K min^{-1} the crystals start to condense and sublime intensely. Sublimates shaped as square rooftiles precipitate on the slide (Fig. 2C) increasing until the temperature reaches the melting point. The crystals and the sublimates melt at 88.5 °C (equilibrium of melting), which coincides with the melting points given in the literature: 88–92 °C (US Pharmacopeia, 2000), 88–90 °C (Merck Index, 1996), 89–92 °C (Pharmacopeia Europaea, 2002). Slowly cooling the melt, mod. I^0 crystallizes after seeding with a high crystallization rate as highly birefringent stems and plates at temperatures above 65 °C. Mod. II crystallizes from the supercooled melt in capillary spherulites being stable between two slides at room temperature for a few weeks (Fig. 2A). On heating mod. II slowly

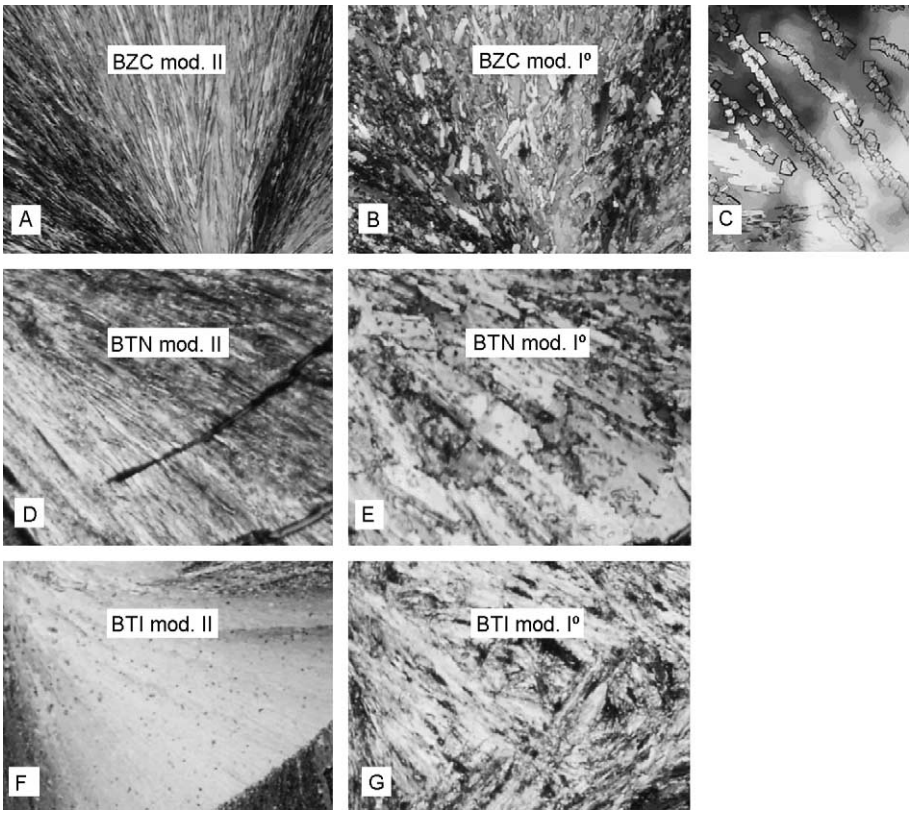

Fig. 2. Micrographs of BZC, BTN and BTI crystal phases: (A) crystal film of BZC mod. II at 40 °C, (B) crystal film of BZC mod. I^0 grown over mod. II at 65 °C, (C) sublimates (mod. I^0) of BZC commercial crystals at 80 °C, (D) crystal film of BTN mod. II at room temperature, (E) crystal film of BTN mod. I^0 grown over mod. II at about 70 °C, (F) crystal film of BTI mod. II at room temperature and (G) crystal film of BTI mod. I^0 grown over mod. II at about 70 °C.

transforms to mod. I^0 at about 65 °C. The transformation mostly starts from the border of the spherulithes, where bright and highly birefringent stems and plates of mod. I^0 grow into the spherulithes of mod. II (Fig. 2B). Probably, the commercial crystals investigated in this study were rapidly precipitated from a saturated quenched solution primarily as mod. II (Ostwald, 1897) and during the storage the crystals transformed to the stable mod. I^0 with the striking secondary texture.

BTN: The melting and crystallization behaviour is closely related to BZC. The highly birefringent crystals of the commercial product scarcely show a secondary texture and the sublimation rate is lower than that of BZC. Mod. II transforms to mod. I^0 at about 45 °C. The shapes of the two phases and the transformation behaviour of BTN are very similar to BZC (Fig. 2D and E).

BTI: The crystals of the commercial product as well as the crystals purified by recrystallization from toluene and from ethanol melt over a larger temperature interval than BZC and BTN. The crystals show neither sublimation on heating nor recrystallization on slow or fast cooling of the melt. Crystallization of mod. II from the supercooled melt only succeeded by seeding with commercial crystals at temperatures between 40 and 60 °C but the crystallization rate is very slow (Fig. 2F and G). Thus, the capability of crystallization is rather low with BTI and the hot-stage microscopic behaviour of the BTI crystals evidently differs from BZC and BTN.

Differential scanning calorimetry—BTN and BTI show very closely related thermal analytical behaviour, whereas the enthalpies of fusion differ a lot. Fig. 3 shows the DSC curves of BZC, BTN and BTI and Table 1 summarizes the thermophysical data. The stable mod. I^0 of all three compounds exhibit an endothermic melting peak (BZC at 88.7 °C, BTN at 57.4 °C and BTI at 54.6 °C) with fusion enthalpies of 20.5 kJ mol^{-1} (BZC), 23.9 kJ mol^{-1} (BTN), 10.7 kJ mol^{-1} (BTI). BZC and BTN can be recrystallized from the melt, whereas BTI does not nucleate at all (see hot-stage microscopy). On cooling the commercial samples using a cooling rate of 5 K min^{-1} a phase transition to the unstable mod. II could be recognized with BTN at 8 °C (0.8 kJ mol^{-1}), with BTI at −10 °C (0.4 kJ mol^{-1}), but not with BZC. Crystallization from the melt directly in the DSC pan was not successful to receive the DSC-curves of mod. II. The unstable modification of BZC only was achievable by crystallization from solvent and shows an endothermic phase transition to the stable mod. I^0 at 81.5 °C with an enthalpy of approximately 1 kJ mol^{-1} (Gruno et al., 1993). Mods. II of BTN and BTI endothermally retransform to mods.

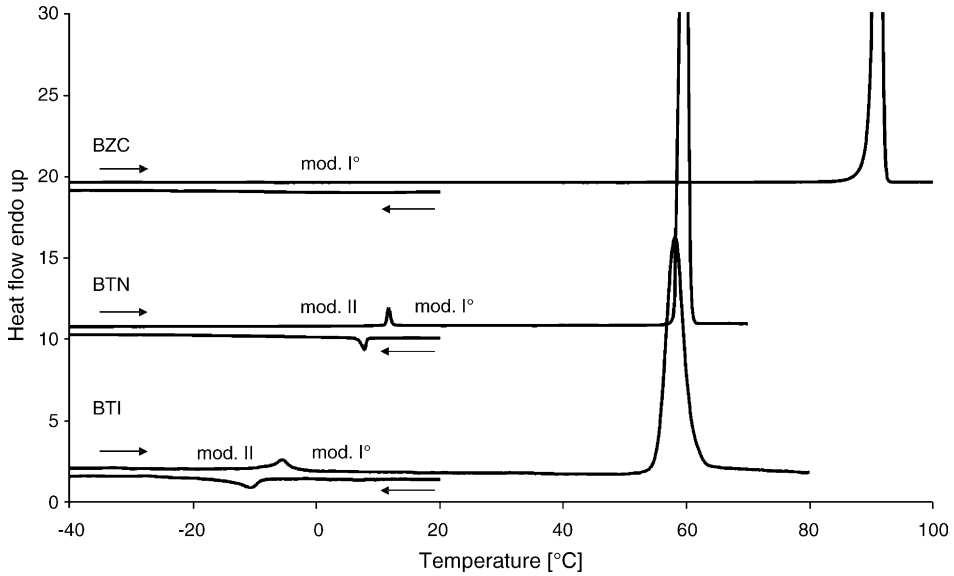

Fig. 3. DSC-curves of BZC, BTN and BTI crystal forms. Measurement cycles started at 20 °C, cooling down to −40 °C and heating up to 70, 80 and 100 °C, respectively. Heating/cooling rates: 5 K min^{-1}.

Table 1
Physicochemical data of BZC, BTN and BTI crystal forms

Compound	BZC		BTN		BTI	
Crystal form	Mod. II	Mod. I^0	Mod. II	Mod. I^0	Mod. II	Mod. I^0
Production	From the supercooled melt and from 1-butanol at −8 °C[a]	Commercial product, from all tested solvents at a.c. and from mod. II by solid–solid transition (HSM)	From the supercooled melt and from mod. I^0 by solid–solid transition (DSC)	Commercial product, from all tested solvents at a.c. and from mod. II by solid–solid transition (HSM, DSC)	From the supercooled melt and from mod. I^0 by solid–solid transition (DSC)	Commercial product, from all tested solvents at a.c. and from mod. II by solid–solid transition (HSM, DSC)
Melting point (°C)		88.7 ± 0.6		57.4 ± 0.4		54.6 ± 0.3
Enthalpy of fusion (kJ mol^{-1}) ±95% c.i.	$21.5_{calc.}$	20.5 ± 0.2	$24.7_{calc.}$	23.9 ± 0.2	$11.1_{calc.}$	10.7 ± 0.1
Transition temperature (°C) (experimental, DSC onset)	81.5[a]		12 ± 0.2		-6 ± 0.6	
	→mod. I^0		→ mod. I^0		→ mod. I^0	
Enthalpy of transition (kJ mol^{-1}) ±95% c.i.	1.0[a]		0.8 ± 0.1		0.4 ± 0.1	
	→mod. I^0		→ mod. I^0		→ mod. I^0	
IR data (cm^{-1}) νNH_2	3407[a]	3410		3396		3378
Order of thermodynamics stability of polymorphs at a.c.	2	1	2	1	2	1
Kinetic stability (storage, 20–25 °C, 30–45% RH)	Few months[a]	Stable	1 day	Stable	1 h	Stable

DSC: differential scanning calorimetry, HSM: hot-stage microscopy, calc.: calculated, c.i.: confidence interval, a.c.: ambient conditions.
[a] Data from literature (Gruno et al., 1993).

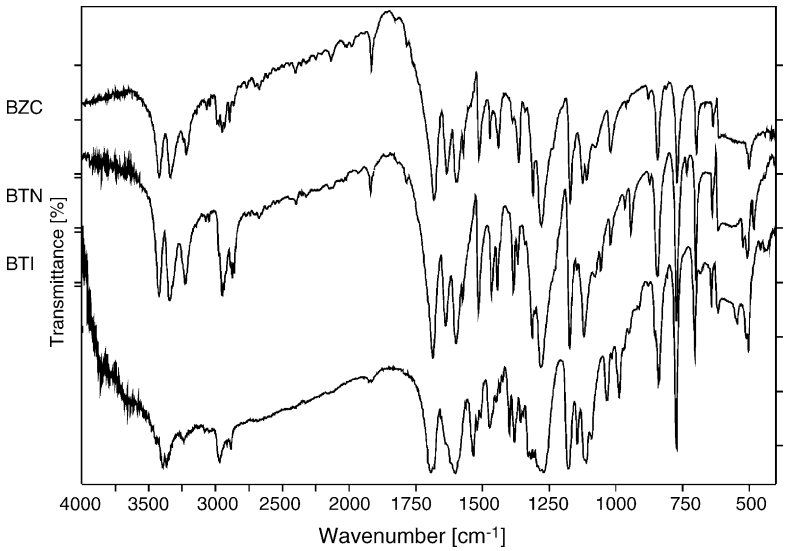

Fig. 4. FTIR-spectra of BZC, BTN and BTI stable crystal forms at room temperature (KBr method).

I^0 in a very small temperature interval at 12 °C (BTN, DSC onset) and −6 °C (BTI, DSC onset), respectively. The enthalpy differences between the polymorphic forms lie between 0.4 and ∼1 kJ mol^{-1}, which are relatively low values compared to other local anaesthetics, indicating similar and low changes within the crystal structure during the phase transition in these three polymorphic systems.

Thermogravimetry did not show significant amounts of residual solvents (<0.04%), but a continuous weight loss due to sublimation could be registered.

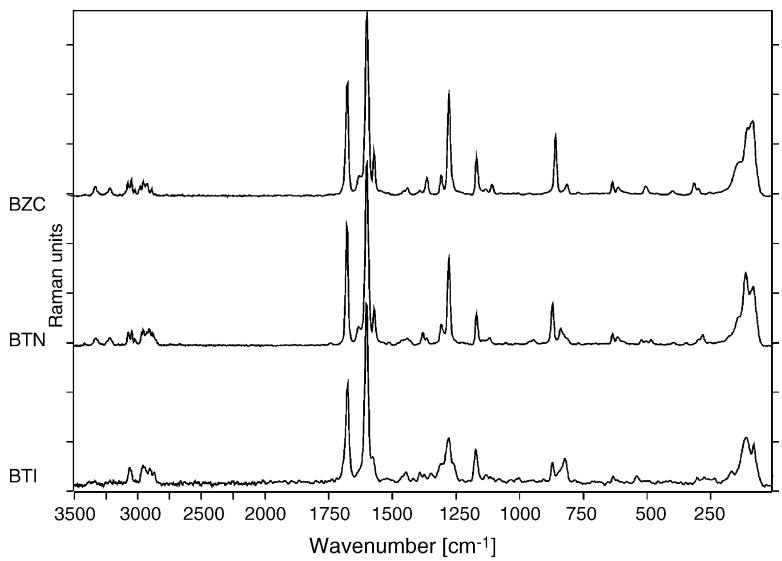

Fig. 5. FT-Raman-spectra of BZC, BTN and BTI stable crystal forms at room temperature.

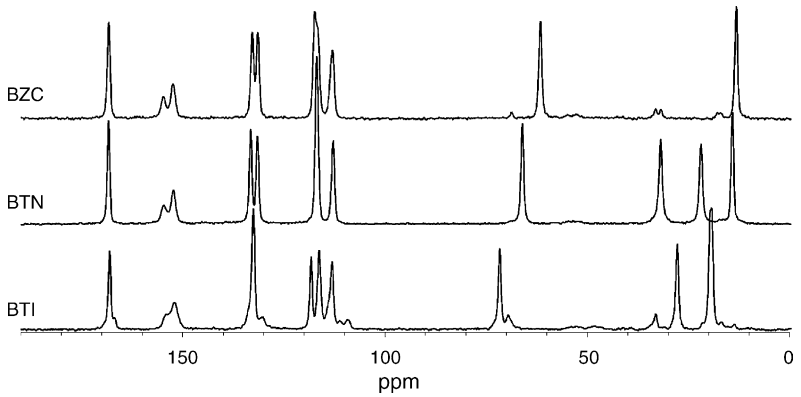

Fig. 6. Solid state ^{13}C NMR-spectra of BZC, BTN and BTI stable crystal forms at room temperature.

3.2.2. Spectroscopy

FTIR- and Raman-spectroscopy: Both, FTIR- (Fig. 4) and Raman-spectra of the stable crystal forms (Fig. 5) show closely related structural composition of the three compounds. With the IR-microscopic method the IR-spectrum of BZC mod. II could be recorded from a thin crystal film between two ZnSe-tablets (not shown). The polymorphs of BZC show minor (band shifts of 3–5 cm^{-1} in average, comparable to other conformational polymorphic LA (Schmidt et al., 2002, 2004)) but well reproducible differences in number and positions of absorption bands. The main differences lie in the range of molecular vibrations (3000–2800 cm^{-1}, FTIR), probably caused by different arrangements of the methylene groups (asymmetric CH-stretching vibrations (Gruno et al., 1993)). Smaller differences were found in the range of νC=O, stretching vibrations of hydrogens of the NH_2 moiety and hydrogen bondings (3450–3220 cm^{-1}, FTIR). The absorption band of the stable mod. I^0 lies at higher wavenumbers as that of mod. II, which evidences a larger entropy for mod. I^0 than for mod. II. The latter is, related to the free-energy curves, the thermodynamic stable form at 0 K. This is consistent with the infrared rule (Burger and Ramberger, 1979) in contrast to many other compounds of local anaesthetic agents (Schmidt, in press-a), which

Table 2
Solid state carbon-13 chemical shifts for the stable crystal forms of BZC, BTN and BTI at ambient probe temperature and solution state carbon-13 chemical shifts from the Daresbury database

Carbon number[a]	BZC		BTN		BTI	
	SSNMR	Database[b]	SSNMR	Database[b]	SSNMR	Database[b]
1	152.4	152.4	152.3	152.4	152.0sh[c]	152.4
2 and 6	113.0; 117.4	116.6	112.8; 116.9	113.5	113.1; 116.3	113.5
3 and 5	131.4; 132.8	131.6	131.5[d]; 133.2	131.6	130.3[d]; 132.5	131.6
4	117.0	116.6	131.5[d]	123.9	130.3[d]	123.9
7	168.3	165.8	168.3	167.0	168.0sh[b]	166.3
8	61.6	60.9	66.0	65.2	71.6	70.9
9	13.2	14.2	31.9	30.8	27.7	27.8
10	–	–	21.9	19.3	19.3; 19.6sh[b]	19.1
11	–	–	14.1	13.7		

[a] See Fig. 1.
[b] UK Chemical Database Service Daresbury.
[c] sh: shoulder.
[d] Assignments uncertain.

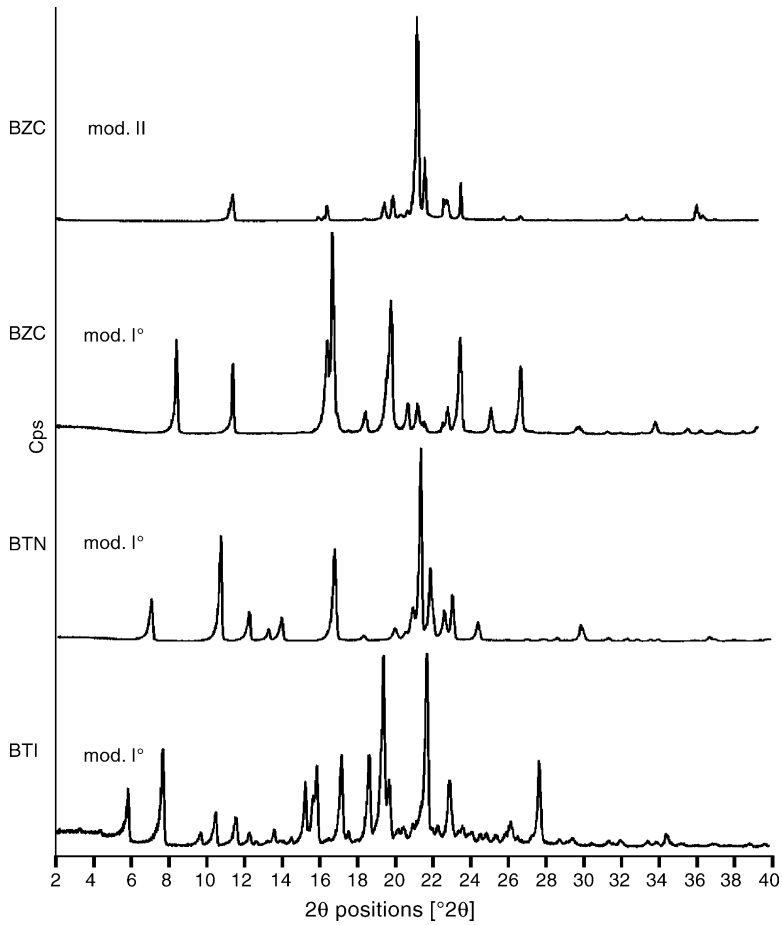

Fig. 7. Powder X-ray diffraction patterns of BZC, BTN and BTI mods. I^0 and BZC mod. II (above) at room temperature. The differences in the peak intensities are attributed to preferred orientation.

Table 3
Most important two theta positions (°2θ), *d*-spacings (*d*) and relative intensities (*I*) of the powder X-ray diffraction patterns of BZC polymorphic crystal forms at 25 °C compared to the values from the literature (Gruno et al., 1993)

h k l[a]	BZC mod. I^0			BZC α[a]			BZC mod. II			BZC β[a]		
	°2θ	*d* (Å)	*I* (%)	°2θ	*d* (Å)	*I* (%)	°2θ	*d* (Å)	*I* (%)	°2θ	*d* (Å)	*I* (%)
0 0 2	8.47	10.43	47	8.52	10.36	24	8.77	10.07	2	8.79	10.05	18
0 1 1	11.59	7.67	35	11.52	7.63	16	11.52	7.68	15	10.57	8.36	3
0 1 3	16.64	5.32	47	16.71	5.30	55	16.66	5.32	8	16.58	5.34	10
0 0 4	**16.94**	**5.23**	**100**	17.02	5.20	74	17.54	5.05	2	**17.66**	**5.02**	**100**
1 0 2	18.75	4.727	12	18.78	4.721	15	18.69	4.74	2	18.31	4.840	14
0 1 4	20.10	4.415	67	**20.16**	**4.401**	**100**	19.76	4.490	10	19.79	4.483	6
1 0 3	21.03	4.220	16	21.10	4.207	29	21.01	4.224	6	20.85	4.257	34
1 0 4	23.88	3.727	48	23.93	3.716	99	23.92	3.718	21	23.98	3.709	87
0 0 6	25.57	3.485	12	25.61	3.476	14	26.23	3.395	3	26.69	3.338	19
1 0 5	27.13	3.284	34	27.19	3.278	68	27.15	3.28	3	27.52	3.239	70
1 0 7	34.46	2.601	7	34.46	2.601	12	27.15	3.28	3	35.35	2.537	14

The highest peak (intensity 100%) is set in bold letters.
[a] Data from literature (Gruno et al., 1993).

violate the infrared rule. Most of the exceptions of the infrared rule found by Burger and Ramberger show an amide moiety, which is missing within the group of ester type LA (and with BZC, BTN and BTI, too). Nevertheless most of the ester type LA violate the infrared rule probably supported by the NH-group in vinyl-position to the carbonyl function. The shift of the νC=O is also seen at 1700 cm^{-1}, FTIR. These findings agree with the suggestion of a layer structure, which causes the phase transformation by modifying the molecular packing.

SSNMR-spectroscopy: Solid state NMR measurements did not show significant differences between the polymorphic forms in all three systems. The ^{13}C-spectra of the stable forms mod. I^0 (Fig. 6) indicate each a single molecule in the asymmetric unit of the three compounds. The ^{13}C chemical shifts and assignments are listed in Table 2 in comparison with the estimated ^{13}C shifts for the solution in DMSO from the SpecInfo database system at Daresbury, UK.

3.2.3. X-ray diffractometry

Powder X-ray diffractometry (PXRD): The X-ray powder patterns of the stable forms of the three bases are illustrated in Fig. 7 and the positions and relative intensities for BZC, compared to the values found in the literature, are listed in Table 3. Comparison of the patterns confirms the samples comprise different polycrystalline structures. BTI commercial and recrystallized samples probably show additional peaks of another system, probably of a (polymorphic) impurity, which is also indicated by the broadened peaks seen in the DSC and IR- and by the multiple peaks in the SSNMR-spectra. The PXRD pattern of BZC mod. II could be recorded after pouring the melt of BZC into the ice-cooled sample holder, where mod. II crystallized immediately. This unstable polymorph shows a crystalline structure completely different from the stable mod. I^0. The positions of the mod. II peaks partly differ from the positions shown by Gruno et al. (1993), but the data are not evident enough to assume that mod. II possibly is a third polymorph of BZC. The differences in the relative intensities are attributed to preferred orientation.

3.2.4. Moisture sorption

The three compounds show no significant absorption of water at relative humidities between 0 and 90% RH, so they can be classified as non-hygroscopic compared to other local anaesthetic compounds of this structural type (Schmidt et al., submitted for publication; Schmidt and Schwarz, 2005; Schmidt, in press-c). The moisture sorption isotherms of the three stable forms are depicted in Fig. 8, which only show a continuous weight loss during the measurement cycle. This effect is independent from the relative humidity of the sample holder, which indicates that the weight loss is caused by sublimation of the crystal compounds (see hot-stage microscopy and TGA).

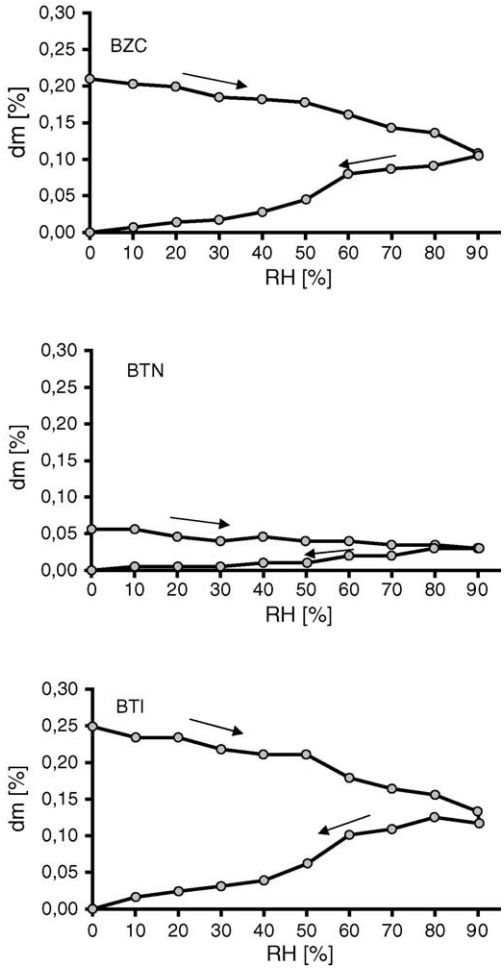

Fig. 8. Moisture sorption isotherms of BZC, BTN and BTI stable crystal forms at 25 °C. The mass change is corrected for the minimum mass value at 0% RH. The measurement cycle started at 0% RH. The whole cycle required about 3 days.

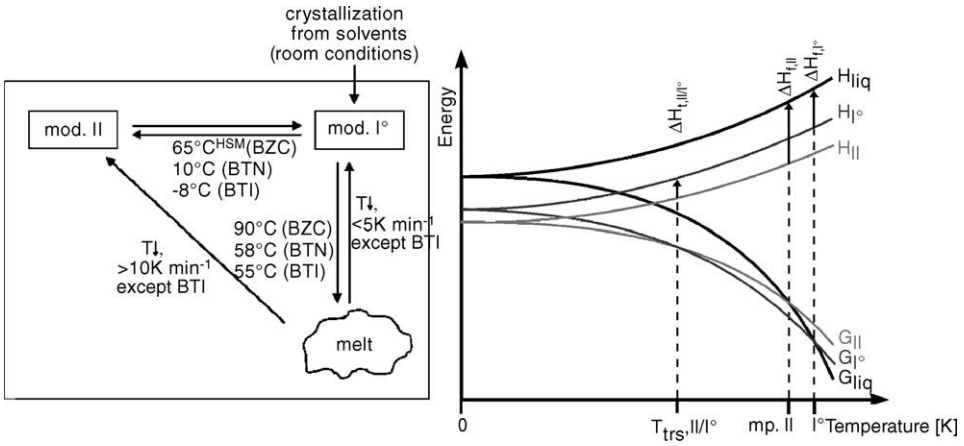

Fig. 9. Flow chart of BZC, BTN and BTI crystal forms and melt with transformation temperatures under ambient pressure conditions (left) and semischematic energy/temperature-diagram of the polymorphs (right). *H* enthalpy, *G* Gibbs free energy, ΔH_f heat of fusion, ΔH_{trs} heat of transition and liq liquid phase (melt). Thermal data from DSC, HSM is the data from hot-stage microscopy.

3.3. Thermodynamic and kinetic stability of BZC, BTN and BTI solid state forms

Table 1 summarizes the most important thermodynamic data of the polymorphs as well as the wavenumbers of the νNH IR-modes of the compounds (intermolecular hydrogen bondings). The thermodynamic relationship of the solid state forms of all three compounds is displayed in the semi-schematic energy/temperature-diagram (Grunenberg et al., 1996) in Fig. 9 along with a scheme showing the possible transition pathways between the forms. Since the mods. II of all three bases transform endothermally to mods. I^0, each of the three pairs of polymorphs are enantiotropically related (heat of transition rule (Yu, 1995)), and thus, the mods. I^0 are the thermodynamically stable forms above their particular transition temperature. Mods. II, which are obtained by recrystallization from the melt (BZC) or by cooling the crystals of mods. I^0 (BTN and BTI), transform to the stable mods. I^0 within a short time (confirmed by DSC) at room temperature. As with other polymorphic local anaesthetics, where the thermodynamically unstable form is only obtainable by cooling the crystalline sample (e.g. pramocaine HCl (Schmidt et al., 2003)), the mods. II of BTN and BTI exhibit a low degree of kinetic stability, and transform to the more stable form rapidly on reheating above the transformation temperature (see DSC). The thermodynamically unstable mod. II of BZC, which is crystallized from a rapidly cooled saturated solution shows a distinctly greater kinetic stability, with the crystals remaining stable for several months (Gruno et al., 1993). This observation supports the results of former investigations on the polymorphism of local anaesthetic drugs examined by us where we came to the conclusion that a crystallization process from a solution or the melt provides these crystalline structures with more kinetic stability than a solid–solid transformation.

4. Conclusions

All of the three local anaesthetics of this study are polymorphic compounds whereas only BZC was known to be dimorphic. The different crystal forms of BZC, BTN and BTI could be identified and proved by thermal analytic and IR-microscopic methods. In all three cases, mod. I^0 is the stable form and present in commercial products. Mods. II crystallize from the supercooled melt, are enantiotropically related to mods. I^0 and thermodynamically stable at temperatures below the thermodynamic transition points. Nevertheless, BZC mod. II, crystallized from solution, exhibits a relatively high kinetic stability (a few months) at ambient conditions. The experimental transition temperatures were found to lie between 45 and 85 °C. Thus, in the syntheses and formulation processes for drug

products of these compounds it is possible to change crystal phases with different physical properties. In order to avoid processing and stability problems associated with unplanned changes in crystal structure, it is important to know in an early preformulation state which of the possible crystal forms are used, which easily can be identified by DSC.

Acknowledgements

The author wishes to thank the European Science Foundation (ESF) and the MORPH network for financial support. Many thanks to Dr. Phuong Ghi and Professor Robin K. Harris for SSNMR measurements, to Prof. Ulrich J. Griesser for directing the research and to Ing. Elisabeth Gstrein for technical assistance.

References

Baptista, A., 1968. Radiocrystallographic study of organic substances. III. Benzocaine. An. Acad. Bras. Cienc. 40, 67–70.

Borka, L., Haleblian, J., 1990. Crystal polymorphism of pharmaceuticals. Acta Pharm. Jugosl. 40, 71–94.

Boyle, M.B., Gikandi, W.W., Gu, Z., Salih, K.S., 2002. Colloidal and Surface Phenomena Aspects of Sunscreen Lotion. Project Report CE457/527, Department of Chemical Engineering, University at Buffalo.

Burger, A., Ramberger, R., 1979. On the polymorphism of pharmaceuticals and other molecular crystals. I, theory of thermodynamic rules. Mikrochim. Acta II, 259–271.

Giron, D., Draghi, M., Goldbronn, C., Pfeffer, S., Piechon, P., 1997. Study of the polymorphic behaviour of some local anaesthetic drugs. J. Therm. Anal. 49, 913–927.

Goodman, H., Gilman, F., 1998. Pharmakologische Grundlagen der Arzneimitteltherapie. McGraw-Hill, Frankfurt, p. 345.

Grunenberg, A., Henck, J.O., Siesler, H.W., 1996. Theoretical derivation and practical application of energy/temperature diagrams as an instrument in preformulation studies of polymorphic drug substances. Int. J. Pharm. 129, 147–158.

Gruno, M., Wulff, H., Pflegel, P., 1993. Polymorphie bei Benzocain. Pharmazie 48, 834–837.

Kofler, L., Kofler, A., 1954. Thermo-Mikro-Methoden zur Kennzeichnung organischer Stoffe und Stoffgemische. Verlag Chemie Weinheim, p. 467.

Kuhnert-Brandstätter, M., 1971. Thermomicroscopy in the Analysis of Pharmaceuticals. Pergamon Press, Oxford, p. 127.

Lindpaintner, E., 1939. Microscopic study of polymorphic substances II. Mikrochemie 27, 21–41.

Lynch, D.E., McClenaghan, I., 2002. Monoclinic form of ethyl 4-aminobenzoate (benzocaine). Acta Crystallogr. E58, o708–o709.

Merck Index, 1996. 12th ed. Merck Research Laboratories, Whitehouse Station, NJ, pp. 182, 249, 878.

Ostwald, W.F., 1897. Studies on formation and transformation of solid materials. Z. Phys. Chem. 22, 289–330.

Pharmacopeia Europaea, 2002. Europäische Arzneibuchkommission, Straßbourg, France, pp. 1271–1272.

Schmidt, A.C. Solid state characterization of chloroprocaine hydrochloride, crystal polymorphism of local anaesthetic drugs, Part VI. J. Therm. Anal. Cal., in press-a.

Schmidt, A.C. Solid state characterization of falicaine hydrochloride and isomorphic dyclonine hydrochloride. Crystal polymorphism of local anaesthetic drugs, Part IV. Eur. J. Pharm. Sci., in press-b.

Schmidt, A.C. Characterization of polymorphs and hydrates of tetracaine hydrochloride. Crystal polymorphism of local anaesthetic drugs, Part IX. J. Therm. Anal. Cal., in press-c.

Schmidt, A.C., Griesser, U.J., Brehmer, T., Harris, R.K., King, A., 2002. Conformational polymorphism of the local anaesthetic drug oxybuprocaine hydrochloride. Acta Crystallogr. A58, 140.

Schmidt, A.C., Niederwanger, V., Griesser, U.J., 2004. Solid state forms of prilocaine hydrochloride. Crystal polymorphism of local anaesthetic drugs. Part II. J. Therm. Anal. Cal. 77, 639–652.

Schmidt, A.C., Schwarz, I., 2005. Solid state characterization of hydroxyprocaine hydrochloride. Crystal polymorphism of local anaesthetic drugs, Part VIII. J. Mol. Struct. 148, 153–160.

Schmidt, A.C., Schwarz, I., Mereiter, K. Polymorphism and pseudopolymorphism of salicaine and salicaine hydrochloride. Crystal polymorphism of local anaesthetic drugs, Part V. J. Pharm. Sci, submitted for publication.

Schmidt, A.C., Senfter, N., Griesser, U.J., 2003. Crystal polymorphism of local anaesthetic drugs. Part I: pramocaine base in comparison with pramocaine hydrochloride. J. Therm. Anal. Cal. 73, 397–408.

Sinha, B.K., Pattabhi, V., 1987. Crystal structure of benzocaine—a local anesthetic. Proc. Ind. Acad. Sci., Chem. Sci. 98, 229–234.

US Pharmacopeia XXIV, 2000. US Pharmacopeial Convention, Rockville, MD, pp. 204–212, 269–270.

Watanabe, A., 2002. Study of crystalline drugs by means of a polarizing microscope. XIX. A trial production of a table of the optical crystallographic characteristics of crystalline drugs including crystal habits. Yakugaku Zasshi 122, 595–606.

Williams, R.O. and Zhang, F., 2003. Topical compositions containing antidepressants and NMDA receptor antagonists for treating pain. US Patent 6,638,981, 27 February.

Yu, L., 1995. Inferring thermodynamic stability relationship of polymorphs from melting data. J. Pharm. Sci. 84, 966–974.

Zhengdong, L., Baichang, W., Genbo, S., 1997. Nonlinear-optical, optical, and crystallographic properties of methyl *p*-hydroxybenzoate. J. Cryst. Growth 178, 539–544.